8-1-2005

Transport and functional behaviour of poly(ethylene glycol)-modified nanoporous alumina membranes

Sang Won Lee
Purdue University

Hao Shang
Purdue University

Richard T. Haasch
Center for Microanalysis of Materials, Frederick Seitz Materials Research Laboratory

Vania Petrova
Center for Microanalysis of Materials, Frederick Seitz Materials Research Laboratory

Gil U. Lee
Birck Nanotechnology Center, Departments of Chemical and Biomedical Engineering, Purdue University,
gl@atom.ecn.purdue.edu

INSTITUTE OF PHYSICS PUBLISHING NANOTECHNOLOGY
Nanotechnology **16** (2005) 1335–1340 doi:10.1088/0957-4484/16/8/059

Transport and functional behaviour of poly(ethylene glycol)-modified nanoporous alumina membranes

Sang Won Lee[1,3], **Hao Shang**[1,3], **Richard T Haasch**[2], **Vania Petrova**[2] **and Gil U Lee**[1,4]

[1] School of Chemical Engineering, Forney Hall of Chemical Engineering, 480 Stadium Mall Drive, Purdue University, West Lafayette, IN 47907-2100, USA
[2] Center for Microanalysis of Materials, Frederick Seitz Materials Research Laboratory, 104 S Goodwin Avenue, Urbana, IL 61801, USA

E-mail: gl@ecn.purdue.edu

Received 21 March 2005, in final form 28 April 2005
Published 7 June 2005
Online at stacks.iop.org/Nano/16/1335

Abstract
The development of hybrid organic–inorganic membranes with a low propensity for protein adsorption and highly uniform nanometre size pores is described. Poly(ethylene glycol) (PEG) monolayers were grafted to nanoporous alumina membranes using covalent silane and physical adsorption poly(ethyleneimine) (PEI) immobilization chemistries. X-ray photoelectron spectroscopy (XPS) and electron microscopy were used to investigate the chemical and physical surface properties of the membranes. The adsorption behaviour of a serum albumin on the membranes was characterized with fluorescence spectroscopy and it was determined that the PEG coating reduced nonspecific protein adsorption to a level too small to be measured. The gas and liquid permeabilities of membranes were measured to determine if the surface chemistries changed the functional behaviour of the membranes. Surprisingly, the silane chemistry produced little change in the permeabilities while polymer adsorption resulted in a total loss of water permeability. The diffusion of ovalbumin through the membranes was also measured and compared with a theoretical value. Diffusion of ovalbumin through the silane-PEG-modified membranes was found to be 50% slower than the unmodified membranes, which suggests that the pores are coated with a dense film of PEG. These results suggest that hybrid organic–inorganic membranes can provide significantly improved functional behaviour over existing organic or inorganic membranes.

Membrane filtration technologies are important for many industrial activities. Due mostly to cost considerations, polymeric membranes are by far the most extensively used type of membranes [1, 2]. However, there has been growing interest in inorganic nanoporous membranes due to their high pore density, narrow pore distribution, and high mechanical strength. Inorganic membranes have become widely used for ultrafiltration and nanofiltration in biotechnology applications, such as separation, bioreactors, tissue culture, and supports for analytical devices [3, 4]. Among these inorganic membranes, anodized alumina membranes have found wide acceptance in the pharmaceutical, food, and electronics industries [5]. Alumina membranes made by anodic oxidation are reported to contain parallel circular pores with a very tight pore size distribution [6]. The pore diameter depends on the applied voltage and can be varied between 20 and 200 nm. The thickness of such membranes is a function of the anodization time and varies between a few tens of nanometres and hundreds of microns.

The transport properties of nanoporous membranes have been intensively studied [5, 7–10]. The well defined pore

[3] These two authors have contributed equally to this work.
[4] Author to whom any correspondence should be addressed.

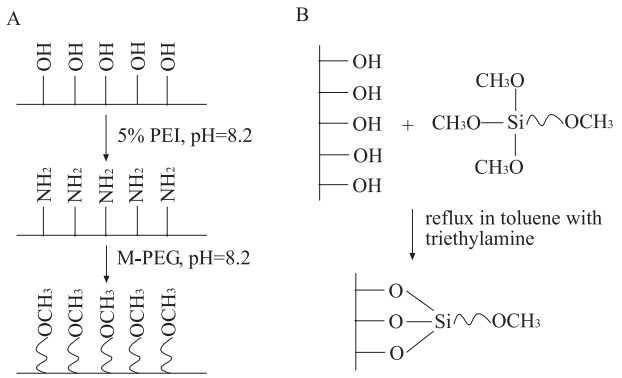

Figure 1. Chemical schemes used to form PEG monolayers on the alumina membranes. (A) The PEI chemistry was a two-step process in which poly(ethyleneimine) was first physically adsorbed on the membrane surfaces. The alumina membranes (Anodisc®, Whatman) were incubated with 5% (w/v) PEI (Polymin SNA, BASF, Rensselaer, NY) in 50 mM Na_2CO_3 at pH = 8.2 for 2 h and excess PEI was removed by rinsing with water (reactions were performed at room temperature unless otherwise stated). The PEI modified alumina surfaces were then reacted with 10 mg ml^{-1} methoxy-terminated PEG succinimidyl propionate (M-PEG, Shearwater, Huntsville, AL) in 50 mM Na_2CO_3 for 2 h at pH = 8.2 and 37 °C. The membranes were rinsed thoroughly and stored under nitrogen until use. (B) The silane chemistry was based on the direct bonding of ω-methoxy-terminated PEG trimethoxysilane to the alumina membrane surface. An anhydrous solution of silane-PEG was prepared in toluene with 5 mM of triethylamine. The membranes were refluxed with the silane-PEG solution in a nitrogen atmosphere for 4 h and then refluxed for another 30 min with pure toluene to remove unreacted silane.

size and structure of these membranes can allow us to apply theoretical models to the transport behaviour of the membrane to identify size-dependent scaling laws. The pore size and surface charge of the membrane have been tuned in many studies. A gold plating technique has been used to precisely control the pore diameter, resulting in the separation of proteins according to their size [11]. Modification of these gold surfaces with charge groups has also been reported to lead to separation of proteins of similar size with different isoelectric points [12]. Modification of these membranes with a self-assembled monolayer bearing carboxyl groups has resulted in separation of bovine serum albumin (BSA) and bovine haemoglobin [13].

The immobilization of hydrophilic polymer monolayers on solids has proven to be an effective method of preventing nonspecific protein adsorption and cell adhesion [14–17]. Among various molecules, PEG is widely used for providing a biocompatible surface due to the hydrophilic and neutral chemical structure of the polymer. PEG chains immobilized on a surface have exhibited the ability to sterically exclude other macromolecules and particles [18]. Experimental and theoretical research suggests that the brush-like PEG monolayers are optimal for preventing protein adsorption, since they provide maximum entropic repulsion between the proteins and surfaces [19]. The grafting of PEG monolayer to alumina membrane surfaces has also been recently studied [20].

In this paper, we describe two surface chemistries that have been developed to graft PEG to the surface of nanoporous alumina membranes and the functional behaviour of the resulting hybrid membranes. Figure 1 presents the two chemical schemes. The poly(ethyleneimine) (PEI) chemistry (figure 1(A)) is a two-step process in which the membranes were first functionalized with high molecular weight PEI providing primary amine groups. In the second step, PEG was grafted to the PEI monolayer through covalent coupling. The silane chemistry (figure 1(B)) is based on the reaction of a ω-methoxy-terminated PEG trimethoxysilane (Shearwater) with the alumina surface forming a self-assembled monolayer. The physical and chemical properties of the hybrid surfaces were characterized with x-ray photoelectron spectroscopy (XPS) and scanning electron microscopy (SEM). The functional behaviours of the membranes were determined using protein adsorption and the transport properties of the membranes.

Table 1. XPS determination of the relative atomic composition and binding energy of specific elements on the unmodified, PEI-modified, PEI-PEG-modified, and silane-PEG-modified alumina membranes.

	Unmodified	PEI-modified	PEI-PEG-modified	Silane-PEG-modified
Al 2p	76.3 eV 53.3%	75.1 eV 16.0%	75.4 eV 6.8%	75.5 eV 9.2%
Si 2p				102.8 eV 1.2%
C 1s: CC, CH	285.0 eV 20.7%	285.0 eV 39.6%	285.0 eV 14.5%	285.0 eV 16.3%
C 1s: C–O	286.9 eV 2.1%		286.4 eV 42.3%	286.5 eV 34.0%
N 1s		397.9 eV 13.4%	400.1 eV 4.5%	397.7 eV 1.2%
O 1s-	528.2 eV 23.9%	528.8 eV 31.0%	528.7 eV 10.0%	527.9 eV 10.9%
O 1s C–O			530.1 eV 21.9%	529.6 eV 27.0%

XPS measurements were conducted using an imaging x-photoelectron spectrometer (Axis ULTRA, Kratos, Chestnut Ridge, NY) equipped with a charge neutralization system. Data were collected using a monochromatized Al Kα source (15 kV, 300 W) at a take-off angle of 60° with respect to the surface. High resolution spectra were acquired using a pass energy of 40 eV, producing an energy resolution of 0.2 eV. For charge neutralization, the low hybrid mode was used with a 200 μm aperture size and 150 W x-ray power. The operating pressure was approximately 10^{-9} Torr. XPS survey and high resolution spectra were collected on the active surface of alumina membranes before and after each of the reaction steps delineated in figure 1. Survey spectra of the as-received alumina membrane revealed significant amounts of aluminium, oxygen, and carbon, and trace amounts of phosphorus and fluorine. The trace elements were removed after the membranes were treated with a concentrated 1:4 H_2O_2:H_2SO_4 solution, while the carbon could only be removed by argon sputtering. Table 1 summarizes the binding energies and relative amounts of the Al 2p, Si 2p, C 1s, N 1s, and O 1s peaks at each reaction step. Identification of specific peaks was complicated by the fact that alumina is an insulator [21]. The C 1s peak measured at 285 eV is attributed to PEI

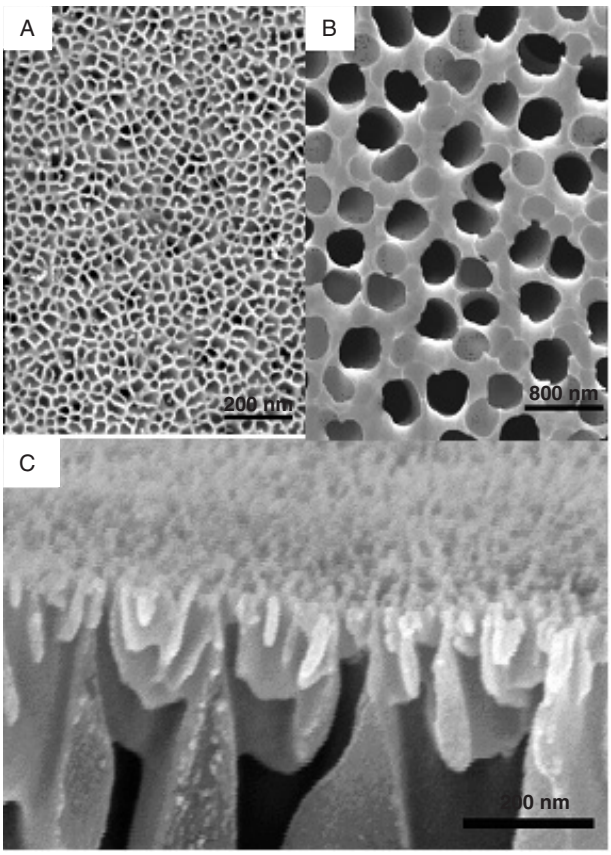

Figure 2. SEM micrographs of the anodically oxidized mesoporous alumina membranes received from Whatman with a nominal 20 nm pore size. The pore size and densities are very different on the (A) active and (B) supporting side. A cross section of a membrane (C) indicates that the active layer is less than 100 nm thick.

and surface contamination while the peak at 286.5 eV is attributed to PEG. The O 1s peaks measured at 528.5 and 530 eV are associated with the alumina membrane and PEG, respectively. Three trends can be identified in table 1. First, the aluminium signal decreases as the membrane is reacted with PEI, silane-PEG, and PEI-PEG, but never drops below 6%. This behaviour is consistent with previous measurements of monolayer films of PEI-PEG and silane-PEG formed on silicon dioxide surfaces [22]. Second, the amount of carbon and oxygen associated with PEG on the PEI-PEG and silane-PEG surfaces was indistinguishable. Third, there was a significant amount of carbon and oxygen contamination on the unmodified membranes even after cleaning. This is attributed to the fabrication process of these commercial membranes.

The structure of the membranes was characterized with field emission scanning electron microscopy (Hitachi S4700). Figure 2 presents SEM micrographs of the active side (figure 2(A)), supporting side (figure 2(B)), and cross-section (figure 2(C)) of the commercial alumina membranes. To minimize charging the membranes were coated with a 3 nm thick Au:Pd (40:60) film using a Emiteck K275 sputter coater at a deposition rate of 20 nm min^{-1}. Figure 2(A) shows that the pores on the 'active surface' are polygonal in shape with a 26 nm average diameter. The pores on the 'supporting side' are circular with an average diameter of 204 nm. The cross-sectional image clearly shows that the large pores transverse most of the 60 μm thickness of the alumina membranes while the 26 nm pores span only approximately 100 nm of the membrane. Table 2 summarizes the mean pore diameter, weighted average pore diameter, pore density, and pore area fraction of the membrane measured from the SEM images. The weighted pore diameter and pore density have been calculated in order to correlate the permeabilities of the membranes with the local hydrodynamic conditions in the pores [3].

Table 2. Summary of the structure of the nominal 20 nm size mesoporous alumina membranes as measured by scanning electron microscopy. The pore diameter (D) is determined from the area (A) of the pore $D = \sqrt{\frac{4A}{\pi}}$ and the weighted average pore diameter is determined from the distribution of pore sizes $\langle D_w \rangle = \sqrt[4]{\frac{\sum_{n=1}^{N} D_n^4}{N}}$, where D_n is the pore diameter and N is the total number of pores. Likewise, pore density and pore area fraction are calculated by counting the number of pores and porous area, respectively, over a series of images.

Surface	Mean pore diameter (nm)	Weighted average pore diameter (nm)	Pore density (pores m^{-2})	Pore area fraction
Active	26	29	6.5×10^{14}	0.37
Support	207	223	1.0×10^{14}	0.37

The anti-fouling behaviour of the membranes was characterized through the adsorption of fluorescein isothiocyanate (FITC) labelled bovine serum albumin (BSA) on the unmodified, PEI-PEG-modified, and silane-PEG-modified alumina membranes. The membranes were soaked in different concentrations of FITC-BSA in phosphate buffered saline solution (PBS) and rinsed with PBS to remove the loosely bound protein. The fluorescence intensity of the wet membranes was quantified using an epi-illumination fluorescence microscope (TE300, Nikon) equipped with a cooled CCD camera (Photometrics Coolsnap HQ, Roper Scientific, Tucson, AZ). Figure 3 shows the fluorescence intensity of the membranes at different FITC-BSA concentrations. BSA adsorption on the unmodified membranes was observed to increase proportionally with the concentration of FITC-BSA up to approximately 1 mg ml^{-1}. Nonspecific adsorption appeared to reach saturation at higher BSA concentrations. This form of adsorption isotherm is consistent with the previous studies of BSA adsorption and has been linked to the formation of monolayer films on both hydrophilic and hydrophobic surfaces, although the total amount of protein adsorbed on the surface has been found to vary significantly [23].

The PEG-modified membranes clearly bind less protein than the unmodified ones. The fluorescence intensity associated with BSA adsorption on PEG-modified membranes was only 10–20% of that on unmodified membranes and the PEI-PEG- and silane-PEG-modified membranes showed similar adsorption profiles at the protein concentration up to approximate 1 mg ml^{-1}. The increased fluorescence intensity observed on the silane-PEG membrane at 2.5 mg ml^{-1} FITC-BSA is attributed to the entrapment of the protein in the pores of the membrane rather than a change in the protein–surface interactions. These results demonstrate that the PEG films are capable of suppressing non-specific protein adsorption to

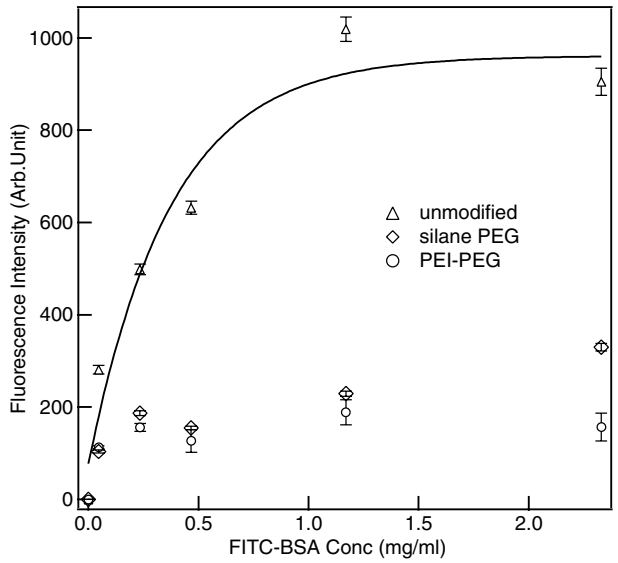

Figure 3. Nonspecific adsorptions on unmodified, PEI-PEG-modified and silane-PEG-modified nanoporous alumina membranes were measured with FITC-labelled BSA. Fluorescence measurements were made at the centre of the membranes, and the standard deviations were assigned based on three measurements.

the membrane surface, which is a striking result considering that the commercial membranes used in this study had a high level of residual carbon on their surfaces. These results imply that these membranes can be used in the complex environments typically found in the biotechnology applications with minimal fouling effects.

The transport properties of liquid, gas, and protein through the unmodified and PEG-modified membranes were studied to determine whether surface modification chemistries influenced the functional behaviour of the membranes. Gas and liquid transport measurements were conducted using nitrogen and water as described previously [3]. The nitrogen and water permeabilities are summarized in table 3. Theoretical permeabilities calculated from the measured pore dimensions and known physical properties of the fluids are also presented in table 3 [3].

The transport behaviour of fluids in nanometre scale pores is known to be highly dependent on the Knudsen number, which is the ratio of the mean free path length of a molecule to the diameter of the pore. Flow changes from slip flow ($0.001 < Kn < 0.1$) to transition flow ($0.1 < Kn < 10$) and finally to molecular flow ($Kn > 10$). For nitrogen flow through 200 nm pores the Knudsen number is of the order of unity, the Reynolds number is less than 10^{-2}, and the Mach number is of the order of 10^{-3}. The flow conditions in the 200 nm diameter pores fall in the transition flow regime. Theoretical analysis of the nitrogen flow through the pores was carried out with a transition regime model developed by Beskok which models flows for multiple regimes [24]. This model predicts that flow rate (Q) scales as

$$Q = -\frac{\pi R^4 \Delta P}{8\,\mu L}(1 + \alpha Kn)\left[1 + \frac{4Kn}{1 - bKn}\right]$$

where ΔP is the pressure drop, R is the radius of the pore, L is the length of the pore, μ is the viscosity of the fluid, Kn is the Knudsen number, α is a function of Kn and $\alpha = 1$ when $Kn = 1$, and $b = -1$. For water flow through a 200 nm pore the Knudsen number is of the order of 10^{-3}, the Reynolds number is less than 10^{-3}, and the Mach number is of the order of 10^{-5}. The flow conditions fall into the continuum-laminar flow regime, which allows flow to be analysed using the well known Hagen–Poiseuille equation.

Table 3. Nitrogen and water permeability for the PEG-modified alumina membranes. The theoretical permeability of nitrogen was calculated using the transition regime model. The theoretical calculation for water permeability was based on the Hagen–Poiseuille equation with modified boundary conditions [31].

	Measured permeabilities (m Pa^{-1} s^{-1})			Theoretical permeability (m Pa^{-1} s^{-1})
Medium	Unmodified	PEI-PEG	Silane-PEG	
Nitrogen	1.98×10^{-6}	7.08×10^{-8}	2.03×10^{-6}	2.61×10^{-6}
Water	7.00×10^{-9}	0	6.59×10^{-9}	4.82×10^{-9}

The measurements of the transport properties of the unmodified and silane-PEG-modified membranes, shown in table 3, are in reasonable agreement with the values predicted using the approximate geometry of the membrane and appropriate flow regime. The permeability of the silane-PEG membranes was indistinguishable from the unmodified membrane in nitrogen and was approximately 8% smaller in water. However, the PEI-PEG modification appears to significantly decrease the permeability of the membranes. That is, a two order of magnitude decrease in nitrogen permeability and total loss in permeability in water was observed even at a pressure of 30 psi. This behaviour suggests that PEI forms a dense film in the membrane pores that reduces the flow of nitrogen and blocks water. The decrease in water permeability through the silane-PEG membranes implies that the PEG decreases the effective pore diameter or increases the effective viscosity of the pore. The fact that the nitrogen permeabilities of the unmodified and silane-PEG membranes are indistinguishable leads us to believe that the silane monolayer does not lead to a large decrease of the volume of pore. However, in water the PEG layer will swell into a monolayer that interacts with water. This suggests that water transport in the pores takes place in two regimes. In the centre of the pore water flows freely while water at the surface of the pore experiences more resistance. This effect can be viewed as a narrowing of the accessible pore diameter.

As a further means of characterizing the transport properties of the membrane, the diffusion of ovalbumin across unmodified and PEG modified membranes was measured using a diaphragm diffusion cell. The membrane was sandwiched between two half U-shaped cells, as described previously [25], which will be referred to as the reservoir and sink. The reservoir contained 50 ml of 100 μg ml^{-1} of ovalbumin in PBS at pH 7.2. The low concentration of ovalbumin used in the reservoir ensures that the molecules are in a monomeric state [26]. Initially, the sink contained 50 ml of PBS buffer. The sink was periodically sampled and the ovalbumin concentration was determined using a micro-BCA assay (Pierce Biotechnology, Rockford, IL). Figure 4 presents the change in the ovalbumin concentration in the sink as a result of its diffusion through the membranes for the unmodified and

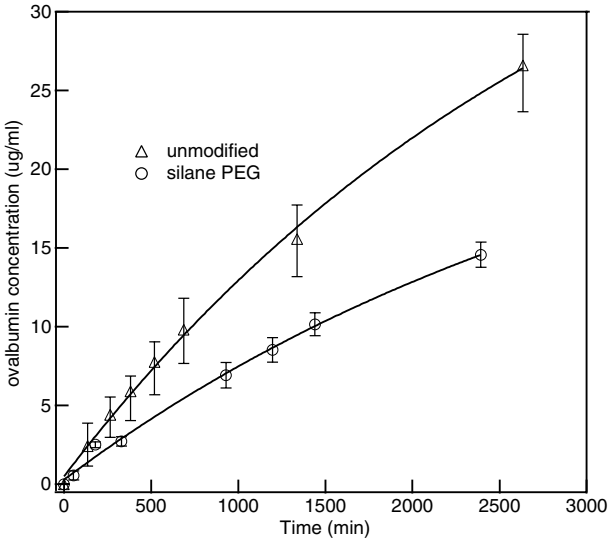

Figure 4. The change of ovalbumin concentration with time in the sink reservoir due to diffusion across an unmodified and a silane-PEG-modified alumina membrane. Standard deviations on the concentration were assigned based on three measurements.

silane-PEG-modified membranes. There was no detectable diffusion of ovalbumin through the PEI-PEG membrane (data not shown).

The diffusivity measurements and theoretical predicted diffusivity are summarized in table 4. The theoretical value was calculated on the basis of the mass balance on the system and the hindered diffusion model [5, 27, 28], in which ovalbumin was treated as a sphere with a 5 nm diameter [26]. This model accounts for the influence of the entrance partition coefficient and hydrodynamic factors associated with the confined diffusion of a spherical solute in a cylindrical pore. Due to the well defined cylindrical shape of the pores, this model can be applied to accurately analyse the ovalbumin diffusivity inside the pores. The dominant resistance that ovalbumin experiences in pores of this size arises from the hydrodynamic interaction of the molecules with the wall of the pore, which includes far field and near field interactions. This model suggests that for the PEG modified membrane that the decrease of the effective pore size will lead to an increase of solute/pore size ratio, which will lead to an increase in the hydrodynamic coupling of the solute with the wall and result in a decrease in the diffusivity of the solute. Unlike water molecules, the PEG layer is not permeable to the ovalbumin because of its size. The pore narrowing effect is more obvious for ovalbumin than for water. This is clearly borne out by the experimental measurement of the diffusivity of ovalbumin through the silane-PEG-modified membrane.

The mass transfer coefficient, which is defined as diffusivity/pore length, was calculated for the supporting layer and active layer, respectively. The mass transfer coefficient of ovalbumin in the supporting layer is around 1.18×10^{-4} cm s^{-1} which is two orders of magnitude smaller than that in the active layer. The thickness of the supporting layer counts for the majority of the resistance that a molecule experienced in transport through the membrane.

The distinguishing feature of the diffusion of the ovalbumin through the silane-PEG-modified membranes is

Table 4. Ovalbumin diffusivity for unmodified and PEG-modified alumina membranes ($\times 10^7$ cm^2 s^{-1}). The theoretical value was calculated based on unmodified membrane using the hindered diffusion model.

Theoretical value	Unmodified	Silane-PEG
7.07	9.00 ± 1.69	4.47 ± 0.33

that the protein flux is significantly lower than that of an unmodified membrane. This observation appears to differ from a previous report which suggests that PEG-modified membranes can suppress fouling, and therefore that high levels of protein transport can be maintained over a longer period of time than the unmodified membrane [11]. We attribute the apparent difference in the performance of the membranes in this study to the fact that the previous study compared PEG-coated membranes with gold-coated membranes. It is highly likely that gold-coated membranes are much more susceptible to fouling than alumina oxide due to the significantly higher Hamaker constant of gold, i.e., the non-retarded Hamaker constants of gold and alumina in water have been reported to be 3.2×10^{-19} and 3.7×10^{-20} J, respectively [29, 30]. It should also be noted that the support layer in this study is responsible for most of the diffusivity resistance in the membranes used in this study and has a pore diameter in excess of 200 nm. Fouling affects these large pores much less significantly than the small pores used by Yu *et al* [11].

This study has demonstrated the effect of PEG modification on the gas, liquid and protein transport properties of nanoporous alumina membranes. Both chemistries produce dense PEG monolayer on the membrane surface. The PEG-modified membranes adsorb significantly less protein than the unmodified membranes. The silane-PEG coating results in the small reduction in permeability of nitrogen and water, while the PEI-PEG appears to block the pores. The silane-PEG modification does appear to coat the inside of the pores and add resistance to water and ovalbumin transport through the membranes. The silane-PEG modification of the membrane results in a 50% decrease in ovalbumin diffusivity compared with the unmodified ones. The decrease in protein flux is attributed to a decrease in the accessible diameter of the pores.

Acknowledgments

This research was supported by the Integrated Detection of Hazardous Materials Program at Purdue University. The SEM and XPS analysis were carried out at the Center for Microanalysis of Materials, University of Illinois, which is partially supported by the US Department of Energy under grant DEFG02-96-ER45439. The authors would like to thank G E Reid, S A McLuckey and M T Griffin for valuable discussions, and D Sherman, N Hovijitra, R Chung and H Patel for their assistance in characterizing the membranes.

References

[1] Baker R W 1991 *Membrane Separation Systems—Recent Developments and Future Directions* (Park Ridge, NJ: Noyes Data Corporation)
[2] Jones C D, Fidalgo M, Wiesner M R and Barron A R 2001 *J. Membr. Sci.* **193** 175

[3] Hovijitra N, Lee S W, Shang H, Wallis E and Lee G U 2004 *Proc. Spie-Int. Soc. Opt. Eng. Chemical and Biological Sensing V (Orlando, Florida)* vol 5416, p 84
[4] Wang Z G, Haasch R T and Lee G U 2005 *Langmuir* **21** 1153
[5] Dalvie S K and Baltus R E 1992 *J. Membr. Sci.* **71** 247
[6] Furneaux R C, Rigby W R and Davidson A P 1989 *Nature* **337** 147
[7] Rigby W R, Cowieson D R, Davies N C and Furneaux R C 1990 *Trans. Inst. Met. Finish.* **68** 95
[8] Martin A, Martinez R, Calvo J J, Pradanos P, Palacio L and Hernandez A 2002 *J. Membr. Sci.* **207** 199
[9] Pradanos P, Arribas J I and Hernandez A 1992 *Sep. Sci. Technol.* **27** 2121
[10] Jirage K B, Hulteen J C and Martin C R 1999 *Anal. Chem.* **71** 4913
[11] Yu S F, Lee S B, Kang M and Martin C R 2001 *Nano Lett.* **1** 495
[12] Chun K Y and Stroeve P 2002 *Langmuir* **18** 4653
[13] Ku J R and Stroeve P 2004 *Langmuir* **20** 2030
[14] Jo S and Park K 2000 *Biomaterials* **21** 605
[15] Arciola C R, Radin L, Alvergna P, Cenni E and Pizzoferrato A 1993 *Biomaterials* **14** 1161
[16] Pekna M, Larsson R, Formgren B, Nilsson U R and Nilsson B 1993 *Biomaterials* **14** 189
[17] Gombotz W R, Guanghui W, Horbett T A and Hoffman A S 1991 *J. Biomed. Mater. Res.* **25** 1547
[18] Harris J M, Martin N E and Modi M 2001 *Clin. Pharmacokinet.* **40** 539
[19] Jeon S I, Lee J H, Andrade J D and Degennes P G 1991 *J. Colloid Interface Sci.* **142** 149
[20] Popat K C, Mor G, Grimes C A and Desai T A 2004 *Langmuir* **20** 8035
[21] Kolics A, Besing A S, Baradlai P, Haasch R and Wieckowski A 2001 *J. Electrochem. Soc.* **148** B251
[22] Metzger S W, Natesan M, Yanavich C, Schneider J and Lee G U 1999 *J. Vac. Sci. Technol.* A **17** 2623
[23] Vandulm P and Norde W 1983 *J. Colloid Interface Sci.* **91** 248
[24] Beskok A and Karniadakis G E 1999 *Microscale Thermophys. Eng.* **3** 43
[25] Hou Z Z, Abbott N L and Stroeve P 2000 *Langmuir* **16** 2401
[26] Matsumoto T, Chiba J and Inoue H 1992 *Colloid Polym. Sci.* **270** 687
[27] Nitsche J M and Balgi G 1994 *Ind. Eng. Chem. Res.* **33** 2242
[28] Deen W M 1987 *AIChE J.* **33** 1409
[29] Luedtke W D and Landman U 1996 *J. Phys. Chem.* **100** 13323
[30] Bergstrom L 1997 *Adv. Colloid Interface Sci.* **70** 125
[31] Gad-el-Hak M 1999 *J. Fluids Eng.* **121** 5